Design, control procedure and start-up of the sCO2 test facility SCARLETT

Flaig, Wolfgang; Mertz, Rainer; Starflinger, Jörg

In: 2nd European sCO2 Conference 2018

2nd European supercritical CO2 Conference
August 30-31, 2018, Essen, Germany

2018-sCO2.eu-106

DESIGN, CONTROL PROCEDURE AND START-UP OF THE SCO2 TEST FACILITY SCARLETT

Wolfgang Flaig*
University of Stuttgart
Stuttgart, Germany
wolfgang.flaig@ike.uni-stuttgart.de

Rainer Mertz
University of Stuttgart
Stuttgart, Germany

Jörg Starflinger
University of Stuttgart
Stuttgart, Germany

ABSTRACT

Supercritical CO_2 (sCO_2) shows great potential as future working fluid for Joule Cycles. Compared to subcritical condition, sCO_2 shows advantages in the heat transfer due to its thermodynamic properties near the critical point, in particular high isobaric heat capacity, fluid-like density and gas-like dynamic viscosity. This can lead to the development of more compact and more efficient components, e.g. heat exchangers and compressors. Current research work at the Institute of Nuclear Technology and Energy Systems (IKE), University of Stuttgart, focuses on a retrofittable, self-propelling and self-sustaining heat removal system for nuclear reactors, based on a sCO2-turbine-compressor system, which is investigated in the frame of the EU-project He-Ro. IKE takes the leading role in the design; manufacturing and testing of a diffusion bonded compact heat exchanger, which enables the decay heat transfer from the reactor loop into the sCO2-cycle. The associated experiments are carried out in the multipurpose test facility, named SCARLETT – **S**upercritical **CAR**bon dioxide **L**oop at IK**E** Stu**TT**gart.

SCARLETT was built up for various experimental investigations of supercritical CO_2 in many different technical fields and is under operation now. It is designed to carry out experimental investigations with mass flows up to 0.110 kg/s, pressures up to 12 MPa and temperatures up to 150 °C.

SCARLETT consists of a closed loop, in which CO_2 is compressed to supercritical state and delivered to a test section. This test sections itself can be exchanged for various investigations. Downstream the test section, the CO_2 pressure will be reduced by an expansion valve and transported back into a pressure vessel, from where it is evaporated and compressed again. In opposite to many other sCO_2-facilities, the application of a high pressure pump or a circulation pump in combination with a pressurizer is refrained for the SCARLETT setup. Instead a piston compressor serves as the central component of the SCARLETT, which is responsible for the rise in pressure upstream the test section. The combined use of a compressor and an expansion valve makes a profound control strategy necessary to achieve constant and stable boundary conditions at the entrance of the test section. Additionally, the operation of SCARLETT is realised in remote control with high-grade automatization. This requires a control program and well-chosen signal routing. In order to support and complement the thermal-hydraulic design as well as the development of the control strategy, a zero dimensional model of SCARLETT was implemented in Matlab, with which the targeted stationary operating points were calculated.

This publication contains the description and the layout of the test facility, as well as the outline of the design. Furthermore the development of the control strategy is explained. Results of the start-up of SCARLETT in non-controlled and controlled mode and the modelling of the stationary operating points will be shown.

INTRODUCTION

The critical point of carbon dioxide (CO_2) is at p = 7.38 MPa and T = 30.98°C [1]. These moderate parameters compared to those of other working fluids like water (p = 22.06 MPa, T = 373.95°C [1]) favor the use of CO_2 as a substitute fluid easier to handle in current research work. Similar to all other supercritical fluids, near its critical point CO_2 shows a significant change in its thermophysical properties. Passing the pseudo-critical point with increasing temperature leads to a massive increase of the isobaric heat capacity and the decrease of the dynamic viscosity. Furthermore, the heat conduction coefficient and the density are initially similar to liquid values and then drop down after passing the pseudo-critical point with

DOI: 10.17185/duepublico/46081

higher temperature. This progression of the properties leads to a high Prandtl Number causing a significant peak in the Nusselt Number and in the heat transfer coefficient, respectively. This leads to high potential as working fluid in heat transfer near the critical point. Figure 1 shows the temperature-dependent progression of the heat transfer coefficient for CO_2, calculated with the Nusselt correlation for heated turbulent pipe flow by Dittus-Boelter [1], shown in Eq. (1):

$$Nu = \frac{\alpha \cdot d_h}{k_{layer}} = 0.023 \cdot Re^{0.8} \cdot Pr^{0.4} \qquad (1)$$

with the Nusselt number Nu, the heat transfer coefficient α, the hydraulic diameter d_h, the conductivity of the boundary layer k_{layer}, the Reynolds number Re, the Prandtl number Pr.

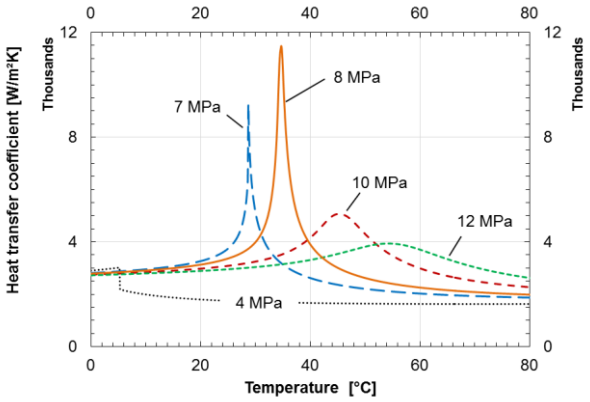

Figure 1: Calculated heat transfer coefficient according to Dittus-Boelter in dependence of the bulk temperature.

Pipe and channel flow under supercritical conditions with intensively heated walls are influenced by the significant change of fluid properties, e.g. density, viscosity, thermal conductivity. In the range of high heat flux combined with lower mass flow densities, the heat transfer strongly depends on heat flux, mass flow and other operation parameters [2]. This may trigger an unexpected and severe rise of the wall temperature, called Deteriorated Heat Transfer (DHT). The reasons for these phenomena are under scientific investigation right now and they are only understood qualitatively [3], [4], [5]. A prediction of the maximum wall temperature occurring under DHT is not possible until now.

Supercritical CO_2 flow with heat transfer has become of great interest lately, because it is suitable as a working fluid for power cycles. Dostal et al. [6] showed the possibility to realise such cycles with high efficiency and reasonable economic capital costs, if efficient and compact components, especially heat exchangers can be applied. But for the dimensioning of compact heat exchangers, it is necessary to know the heat transfer mechanisms and to obtain quantitative predictions of the necessary heat transfer. Different scientific research work focuses on a passive safety system based on a supercritical CO_2-Brayton cycle for nuclear reactors. This system is self-sustaining as well as self-propelling and able to transform the nuclear decay heat into waste heat, which will be emitted to the environment [7]. The components of this passive safety system have to be tested and numerical models for existing simulation programs have to be improved. The necessary software is partly developed, but there is still lack of experimentally validated models. In this context diffusion bonded plate heat exchangers (DBHE) as special type of compact heat exchanger are of great interest [8]. The technology seems very promising, particularly if supercritical CO_2 is used, because high heat transfer power is achievable, both on the pseudo-evaporation side and the pseudo-condensation side [9], [10].

TEST-FACILITY 'SCARLETT'

At Institut für Kernenergetik und Energiesysteme (IKE), a multipurpose test facility, named SCARLETT – **S**upercritical **CAR**bon dioxide **L**oop at IK**E** Stu**TT**gart, has been built for numerous investigations of supercritical CO_2 and is now in operation (Figure 2). This facility enables various experiments for fundamental research and applied science with supercritical CO_2. Separate test sections, which can be installed easily, provide a great variety of experimental investigations. The emphasis of the investigations will be on the validation of numerical flow simulations with supercritical fluids and the gathering of experimental data for validation of numerical simulations. The acquired knowledge and data will be used both in the nuclear field, and for non-nuclear applications, like low-temperature heat transfer, waste heat utilization, renewable energy sources and refrigeration engineering.

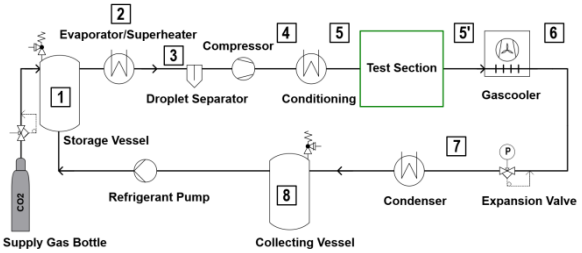

Figure 2: Scheme of the test facility SCARLETT.

Selection of Boundary Conditions. The layout data of the supercritical recompression cycle according to Dostal [6] are used as guideline for the testing facility. The high-pressure side is operating at a pressure of 20 MPa. Under these conditions, CO_2 shows a gas-like flow behavior, far off the critical point, which is not of interest for investigations about the special heat transfer phenomena. The low-pressure side in this cycle works with a pressure of 7.7 MPa and in a temperature range from 32 to 69°C for the precooler, and 69 to 157°C for the low-temperature recuperator. These conditions are near to the critical point and the base for future investigations. For a downscaled 1 MW cycle the mass flow is calculated to 11.9 kg/s. After the comparison of a typical compact heat exchanger [11], the mass flow has to be about 0.122 kg/s for the precooler and 0.027 kg/s for the low temperature recuperator. This

DOI: 10.17185/duepublico/46081

prototype allows the investigation of max. 30-50 channels per layer on a basis of max. 220 mm × 220 mm. This means a step forward compared to the investigations of Kruizenga et al. [12], who tested nine parallel channels.

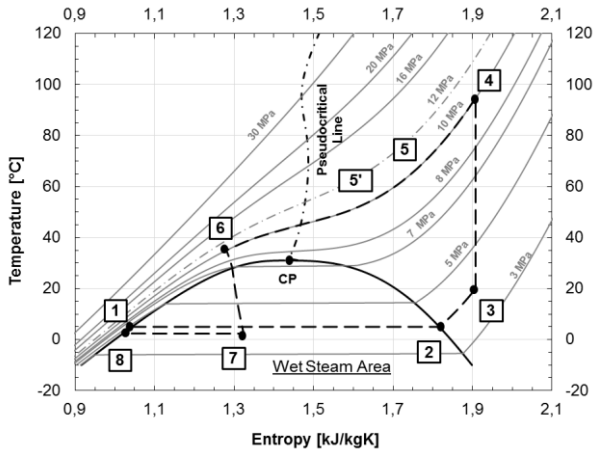

Figure 3: Temperature-entropy-diagram of the SCARLETT process.

In comparison to other sCO_2 facilities, the mass flow will not be compressed to supercritical pressure by a gear-pump or a membrane-piston-pump. Instead, a piston compressor is applied, also used by commercial refrigeration plants with a maximum mass flow of about 0.110 kg/s. This type of compressor limits the maximum achievable pressure to 14 MPa. In the SCARLETT facility, it will be possible to investigate several layers of a compact heat exchanger, which makes an appropriate value of the mass flow more import than a high pressure level. Hence, a maximum operation pressure of 12 MPa provides a suitable operation margin to the maximum pressure achievable. All other components are designed for a maximum pressure of 20 MPa, so that after an upgrading stage of the facility, a more powerful compressor can be implemented which is able to provide higher pressure up to 20 MPa.

The compressor outlet temperature of up to 160°C makes it necessary to cool the mass flow massively to work with lower test temperatures. Therefore, high thermal power has to be dissipated, which makes an adequate cooling system necessary.

The operating parameters of the facility are shown in Table 1. The power class of the planned facility fits to international existing research cycles with supercritical CO_2, e.g., cycles for fundamental research with lower mass flow but similar pressure level [10], [13] and [14]. There is also a CO_2-cycle at the University of Wisconsin, Madison for investigations on compact heat exchangers [15]. The maximum pressure of this cycle is higher (20 MPa vs. 12 MPa) but the mass flow is lower (0.015 kg/s vs. 0.110 kg/s).The test facility SCARLETT is smaller compared to the large cycles, which are used by the US Department of Energy (DOE) [16]. The cycle at the Bhaba Atomic Research Centre, Mumbai, is of interest regarding natural convection investigations with supercritical CO_2 [17]. The size and research capacity of SCARLETT fits well between the very small, single effect test facilities and the large power cycle facilities, closing this gap.

Table 1: Available experimental parameters for SCARLETT.

Parameter	Symbol	Value	Unit
Mass flow rate	$\dot{m}_{sCO_2}$	13-110	g/s
Temperature	T	5.0-150	°C
Pressure	p	7.5-12.0	MPa
Inner pipe diameter	d_i	10.0	mm

Facility Design. The technical objective of SCARLETT is to provide supercritical CO_2 at predefined temperatures and pressures to the test sections. This allows investigations in many different technical fields. Therefore, the facility is designed as a closed loop, in which CO_2 is circulating continuously. To fulfill this claim there are commonly used two types of basic facility designs in laboratory scale to shift CO_2 to the supercritical state [9], [12]. One type is using a stand-alone high pressure pump to raise the pressure, whereas the other type is consisting of a circulation pump in combination with a booster pump or a nitrogen pressurizer to hold the pressure and is applied in most cases. A third type uses a compressor and is similar to a refrigerant plant cycle. The advantage of this cycle is the availability of components and the operating efficiency of the compressor in the predefined pressure and mass flow range. Due to these reasons the compressor type facility design was chosen.

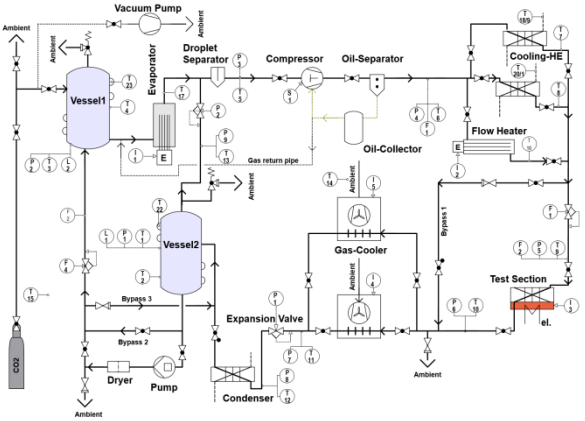

Figure 4: Piping and instrumentation diagram of the test-facility (according to EN ISO 10628).

If the SCARLETT facility is off-state, the CO_2 is stored as liquid in two pressure vessels, the storage vessel and the collecting vessel. The storage vessel can be refilled by CO_2 gas (standpipe) bottles. During operation the CO_2 passes through the SCARLETT facility, shown in Figure 2. First, it flows through an electrical heated evaporator, in which it will be isobarically evaporated and overheated of about 10 K to ensure a minimum of remaining liquid droplets in the CO_2 gas flow. After passing a droplet separator, for eliminating the last liquid droplets and to prevent the compressor from damages by liquid

DOI: 10.17185/duepublico/46081

strike, the CO_2 will be surged by a piston-compressor and compressed to supercritical pressure and temperature. Depending on the pressure ratio, outlet temperatures from 80 to 160°C are possible. After the compressor, the supercritical CO_2 flows through a heat exchanger, where it is either cooled or heated to the pre-defined test temperature (so called conditioning).

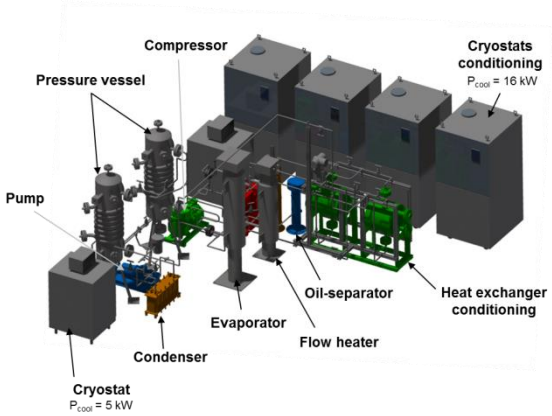

Figure 5: CAD-sketch of the test-facility SCARLETT.

At this point, the SCARLETT facility provides a user defined mass flow of sCO_2 at defined pressure and defined temperature to the test section, in which the experiments will be carried out. Because of the various conceivable investigations in the test section, it is illustrated as a box in Figure 2, which shows the scheme of the CO_2 loop. After leaving the test section the CO_2 is cooled to ambient temperature in a forced-ventilation gas cooler that is installed outside the laboratory building. Downstream of the coolers an expansion valve reduces the CO_2 pressure in an isenthalpic process to subcritical conditions into the wet steam area. Afterwards, the CO_2 is fully isobarically condensed in a plate heat exchanger and flows into the collecting vessel. A refrigeration pump installed between both pressure vessels delivers the liquid CO_2 back into the storage vessel closing the loop.

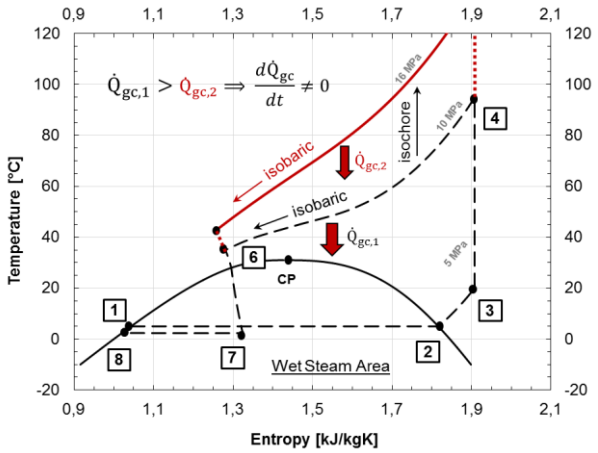

Figure 6: Influence of a transient on the SCARLETT process.

The thermodynamic cycle of the testing facility is plotted in Figure 3 by a temperature-entropy-diagram. In Figure 4, the detailed piping and instrumentation diagram of the facility is presented. Figure 5 shows a CAD-sketch of the CO_2 facility SCARLETT including peripheral components and the laboratory. Figure 7 shows pictures of the facility.

The test facility works similar to a refrigerant plant, this means, there are certain factors which influence the stationary behavior and thereby the experimental parameters, e.g. frequency of the current supplying the compressor, degree of opening of the expansion valve, coolant temperature at the inlet of the condenser, ambient temperature, speed of the gas cooler fan, conditioning cooling power. A variation of at least one parameter induces a temporary transient which leads finally to the adjustment of different stationary experimental parameters. This is exemplarily explained for a reduction of the gas cooler power (triggered by a higher ambient temperature e.g.) in Figure 6. The pressure raises after an isochoric change of state on the high pressure side due to the constrained heat power emission. The mass flow rate subsequently decreases due to the characteristic of the piston compressor. This has to be taken into account for the design and predicting of the stationary operating points.

The primary design equation is derived from an energy balance (Eq. (2)) and applied on heat transferring components, like heat exchangers, evaporator and condenser.

$$\dot{Q}_{HT} = \dot{m}_{sCO_2} \cdot \left(h_{in}(T,p) - h_{out}(T,p)\right) \qquad (2)$$

with the heat transfer rate $\dot{Q}_{HT}$, the sCO_2-mass flow $\dot{m}_{sCO_2}$, the specific enthalpy $h_{in}(T,p)$ at the entrance and the specific enthalpy $h_{out}(T,p)$ at the outlet of the component.

Figure 7: Current picture of the test-facility SCARLETT with an integrated experiment.

Furthermore the actual achievable heat transfer rate is given by Eq. (4) and linked with Eq. (3) to calculate the necessary heat transferring area.

$$\dot{Q}_{HT} = \alpha \cdot A \cdot \theta_{log} \qquad (3)$$

DOI: 10.17185/duepublico/46081

with heat transfer coefficient α, the heat transfer area A and the mean logarithmic temperature Θ_{log}.

The ejected mass flow of the compressor is not constant. It depends on the pressure ratio Π (high pressure p_1 to low pressure p_0) and the CO_2 density at the inlet of the compressor, according to Eq. (5):

$$\dot{m}_{sCO_2} = n \cdot V_{pd} \cdot \rho_0(T_s, p_0) \cdot \lambda(\Pi) \tag{4}$$

with the rotational speed n, the piston displacement V_{pd}, the density of the suction gas ρ_0 and the delivery rate λ.

The rotational speed can be calculated again by the effective frequency of the 3-phase current f_c and the number of magnetic poles in the induction motor m according to Eq. (5):

$$n = \frac{f_c}{m} \tag{5}$$

The change of state caused by the expansion valve is of isenthalpic nature. The induced pressure drop is calculated by Eq. (6).

$$\Delta p_{EV} = (p_1 - p_0) = \frac{1}{\rho_m} \cdot \left(\frac{\dot{m}_{sCO_2}}{K_V}\right)^2 \tag{6}$$

with the pressure drop of the expansion valve Δp_{EV}, the mean sCO_2 density between inlet and outlet ρ_m and the flow coefficient of the expansions valve K_v.

The outlet temperature and steam quality can be calculated with help of the CO_2 properties, delivered by Refprop , when p_0 and p_1 are known.

In order to receive a definite system of equations, Eq. (7) is applied, which considers that a change of the operating point of the facility induces a relocation of CO_2 mass from low pressure to high pressure side or vice versa.

$$\frac{dm_{HP}}{dt} = -\frac{dm_{LP}}{dt} \Rightarrow \frac{d\rho_{HP}(T,p) \cdot V_{HP}}{dt} = -\frac{d\rho_{LP}(T,p) \cdot V_{LP}}{dt} \tag{7}$$

with the total CO_2 mass on the high pressure and low pressure side $m_{HP/LP}$, as well as the density and the volume on both sides $\rho_{HP/LP}$, $V_{HP/LP}$.

Experimental results show, that the temperature of the coolant fluid (water/glycol mixture) on the secondary side of the condenser is affecting the CO_2 temperature and the corresponding CO_2 vapor pressure p_0 on the low pressure side. To simplify the calculations, $_{p0}$ can be assumed by the coolant temperature.

The pressure drop in the pipe is estimated by Eq. (8):

$$\Delta p_{Pipe} = \frac{1}{2} \cdot \dot{m}_{sCO_2}{}^2 \cdot f \cdot \frac{L}{A_{Pipe}^2 \cdot d_i \cdot \rho} \tag{8}$$

with the pressure drop of the expansion valve Δp_{EV}, the Darcy friction factor f, the length of the pipe L, the cross sectional area of the pipe A_{pipe} and the fluid density ρ.

The Darcy friction factor is calculated according to Colebrook for turbulent flow.

These equations were implemented in *Matlab* and used for a zero-dimensional model to design, predict and analyze the steady state behavior of the facility.

Mechanical stress of pressurized components is calculated according to standard DIN EN 13445-3 [18].

Oil Recirculation System. A piston compressor needs lubrication oil for preventing the compressor from mechanical damage, such as piston seizure. Refrigeration-machine oil based on Polyalkylenglykolen (PAG) is used according to the recommendation of the compressor manufacturer. The decomposition temperature of this oil is 180°C, which suits well to the maximum temperature of the compressor.

Part of this oil is entrained into CO_2, especially at supercritical state. Dang et al. [19] showed, that in experiments with oil concentrations of more than 1 %, pure oil is enriching at the tube walls, dissolving liquid CO_2 and subsequently influencing the pressure drop and the heat transfer significantly. In order to reduce these effects, an oil recirculation system is installed in SCARLETT, which is shown in Figure 4. This system works as follows:

An over-dimensioned coalescence separator is installed in the main pressure gas pipe right after the compressor. It extracts more than 99 percent of the oil from the sCO_2 gas flow. Additionally it serves as a buffer volume to smoothen inevitable oscillations that are deriving from the piston displacement. The removed oil, together with partly gaseous CO_2, flows into an oil collector vessel. The CO_2 fumes upwards and is released into the low pressure side of the test facility through a bypass pipe and a check valve. In case of an oil low level signal at the oil sump of the compressor, a magnetic valve opens and the oil flows back from the collector to the compressor, driven by pressure gradient. The remaining oil concentration will be obtained by a weighting procedure as described by Dang et al. [19]

Controlling. To obtain the user-given test condition at the entrance of the test-sections, the facility has to reach and stabilize defined operation parameters, i.e. temperature, pressure and mass flow. To fulfill this requirement, it is necessary to control all three parameters during operation. Because of the mutual influence of the parameters on each other, a decentralized Multi-Input-Multi-Output (MIMO) control strategy was chosen. This means temperature, pressure and mass flow are regulated by separate PID-controllers. The pressure is set by the flow resistance of the expansion-valve and the temperature by the cooling power of the cryostats supplying the conditioning heat exchanger. The mass flow can be varied by the rotation speed of the compressor engine, which is induced by a frequency converter. The main functions for the controlling and surveillance are concentrated in one program,

DOI: 10.17185/duepublico/46081

created by the software *Agilent-Vee*. All components are remotely controlled by this program processing analog or digital signals (hexadecimal code in complement representation) via serial ports. Eq. (9) shows the law of controlling for a PID.

$$u(t) = K_p \cdot \left(e(t) + \frac{1}{T_N} \cdot \int_0^T e(t)\, dt + T_{vh} \cdot \frac{de}{dt} \right) \qquad (9)$$

with the time continuous set value *u(t)*, the time continuous control deviation *e(t)*, the proportional control amplification K_p, the reset time T_N and the lead time T_{Vh}.

In order to implement a PID into the digital program, it has to be discretized by z-Transformation. Applying the difference rule afterwards leads to the position-algorithm in Eq. (10), which is calculated my means of measurement data to set the values for the expansion valve and the frequency converter.

$$\begin{aligned} u(k) = u(k-1) + e(k) \cdot \left(K_p + \frac{K_p \cdot \Delta t}{2 \cdot T_N} + \frac{K_p \cdot T_{vh}}{\Delta t} \right) \\ - e(k-1) \\ \cdot \left(K_p - \frac{K_p \cdot \Delta t}{2 \cdot T_N} + \frac{2 \cdot K_p \cdot T_{vh}}{\Delta t} \right) + e(k \\ - 2) \cdot \left(\frac{K_p \cdot T_{vh}}{\Delta t} \right) \end{aligned} \qquad (10)$$

with the time discrete set value *u(k)* and the time discrete control deviation *e(k)*.

The PID controllers for pressure and mass flow have been implanted digitally within the software *Agilent Vee*. In order to guarantee sufficient controlling quality, the pressure and mass signals have been investigated by a Fourier-transformation to detect the dominant frequencies. No relevant frequencies above 0.1 Hz were registered, which means that the clock cycle time of the Agilent system of 1.2 s is sufficient to fulfill the Nyquist-Shannon- sampling-theorem. Furthermore the integration time of the pressure and mass signal is raised on 100 net cycles to avoid aliasing.

The PID controller for the temperature is designed as an analog device, which is integrated into the cryostats and will set the temperature of the cooling fluid according to Eq. (9) as well.

Measurement Techniques. To control the test SCARLETT facility, several measurement instruments are available. All sensors are connected to an *Agilent 34980a* data acquisition system, which allows sending and receiving data to and from analogue devices. Table 2 gives an overview of the applied measurements instruments and their measuring range and their accuracy, respectively. Besides the described measurement devices, an observation window will be installed to enable optical measurements.

Table 2: Measurement devices applied in SCARLETT.

Parameter	Device	Range	Accuracy
Mass flow rate	Coriolis	13-130 g/s	0.5%
Temperature	Pt-100	-20-200 °C	0.15+0.002 T
Pressure	Piezoresistive	0-20 MPa	0.15%
Liquid-level	Difference Pressure	0.2-1 m	0.075%

Safety Installations. The threshold limit value of CO_2 at working place is 5000 ppm, defined for German workplaces by the German Government at TRGS 900 [20]. CO_2 is toxic for humans in concentration higher than 5 % of the breathing air. Furthermore, the high pressure in the facility can possibly be a safety risk in the case of a failure of single components. However, to ensure best possible safety for employees in the CO_2-laboratory, there are several arrangements, which have been applied to the operation of the facility:

- Gas detection devices to warn of a dangerous concentration of CO_2.
- Exhaust extraction system to maintain a low level of CO_2 concentration in the air.
- Inhabitancy in the CO_2-laboratory during operation is not permitted. Instead, the laboratory will be controlled from an adjacent laboratory.
- Safety valves are installed in the low- and high-pressure side to exclude an undue pressure peak. Furthermore, pipes flown through by liquid CO_2 are not lockable or equipped with safety valves.
- The controlling software is operating the facility with a minimum of human interventions. Especially, temperatures and pressures are surveilled steadily. Invalid values are countered automatically by shutting down the compressor and opening the expansion valve.
- Safety shutdown of compressor, evaporator and heaters via relays if there is no signal received from the controlling software for more than 10 s.

The complete facility is constructed according to the European Pressure Equipment Directive (guideline 97/23/EG) [21] and the standard (DIN EN 378) for refrigerating plants [22]. It has been certified by the German Technical Control Board (TÜV, Technischer Überwachungsverein).

RESULTS

The start-up of the test facility includes the implementing and testing of the controllers and the controlling software while bypassing the test section. The main measurement campaign concerning pressure loss and heat transfer of the DBHE is finished.

Start-Up of the Test-Facility. Figure 8 shows the compressor curve, derived by several experiments. The mass flow emitted by the compressor depends on two parameters, the compression ratio (high pressure to low pressure) and the

DOI: 10.17185/duepublico/46081

temperature of the condensate, which corresponds directly to the suction pressure. This means that an increasing test pressure (included in the compression ratio) influences the mass flow reciprocally, which is typical for a piston compressor. This result is emphasized by Eq. (6) for calculation of the emitted mass-flow of a piston compressor.

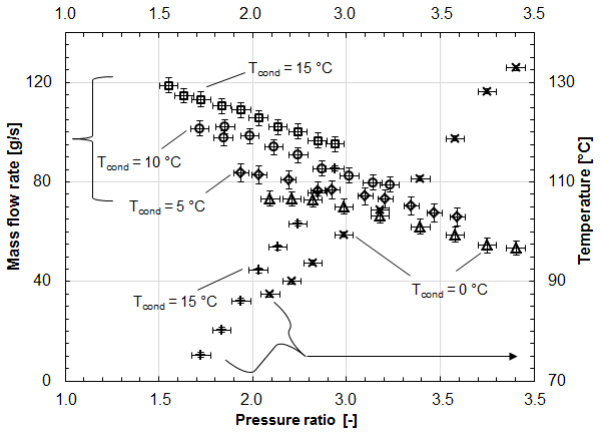

Figure 8: Characteristic line of the compressor Bitzer 4PTC.

Although the piston displacement is constant, the mass filling out this volume in one rotation depends on the density of the suction gas (depends on superheating temperature and low pressure again) and is inhibited by the delivery rate. The delivery rate takes mass loss and the decreasing of the density inside the compressor into account, which is mainly induced by a higher pressure ratio. Figure 8 shows furthermore that the emitting temperature of the compressor is raising with higher pressure ratio, with a lower temperature of the condensate or with lower suction pressure. This leads to the need to control the cooling power of the cryostats on the secondary side of the conditioning during operation as well.

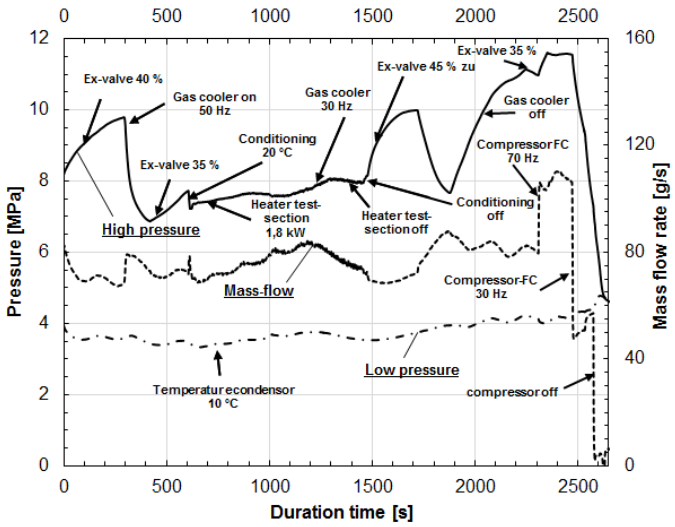

Figure 9: Process uncontrolled.

The described characteristic behavior of a compressor leads to an unsteady temporal behavior of the test pressures and the mass flow rate (like it is in a non-controlled refrigerant cycle), as can be seen in Figure 9. The pressure and mass flow rate are strongly influenced by several parameters like the rotation speed of the gas cooler fan, the condensing temperature, the cooling power and temperature in the conditioning and the heating power and temperature in the test-section.

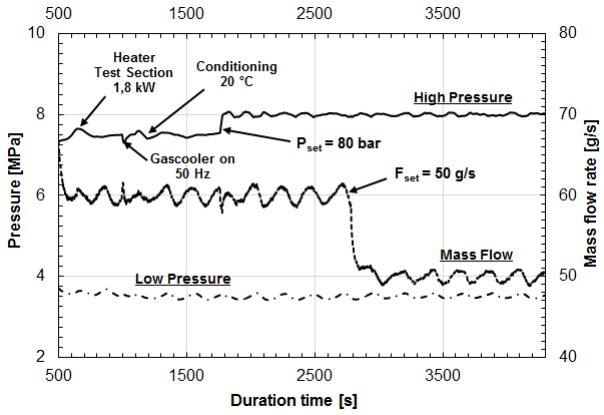

Figure 10: Process controlled.

The mass flow rate and the pressure are stabilized by changing the rotation speed and varying the opening of the expansion-valve, respectively, which is the task of the digital controllers. The results are shown in Figure 10, where the time–depended behavior of the control parameters pressure and mass flow rate can be seen, while PID-controllers are activated. Even under influence of disturbance value, like advanced heat emission at the gas cooler by starting the fan, the pressure and mass flow rate is constant and the disturbance suppressed by the controllers. After changing the set-points, the pressure and the mass flow rate are changing fast and continuously, confirming a reasonable operation of the facility by the settings of the controllers.

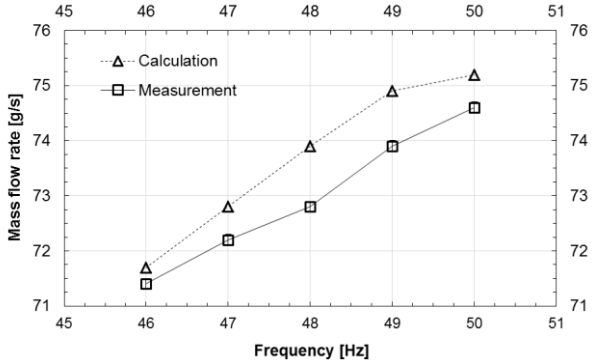

Figure 11: Dependency of the mass flow rate on the frequency of the compressor engine.

DOI: 10.17185/duepublico/46081

Figure 11 to Figure 13 show the comparison between the calculation, done for the SCARLETT design and the measurements of stationary operating points regarding exemplarily the mass flow rate. Figure 11 is dedicated to point out the influence of the 3-phase-frequency on the mass flow rate. Furthermore Figure 12 shows the effect of varying the degree of opening of the expansion valve on the mass flow rate. Figure 13 features the impact of the coolant temperature at the inlet of condenser on the mass flow rate.

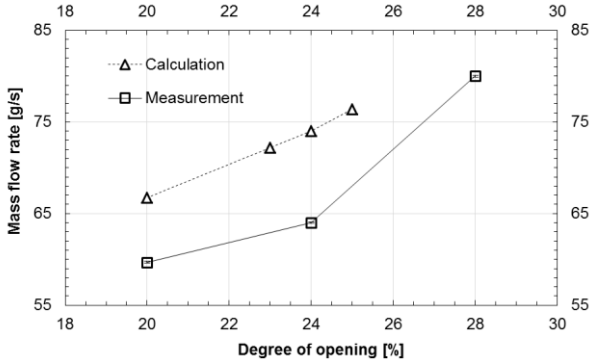

Figure 12: Dependency of the mass flow rate on the degree of opening of the expansion valve.

All three cases show a sufficient congruence between calculation by the zero dimensional *Matlab* model and the experimental data. The process of the mass flow rate during a variation of the influence parameters frequency, coolant temperature and degree of opening of the expansion valve is displayed well by the model. The quantitative accordance is given in general. The discrepancy between the calculated and the measured mass flow rate is less than 10 g/s in all three cases and less than 5 g/s for a variation of coolant temperature and frequency.

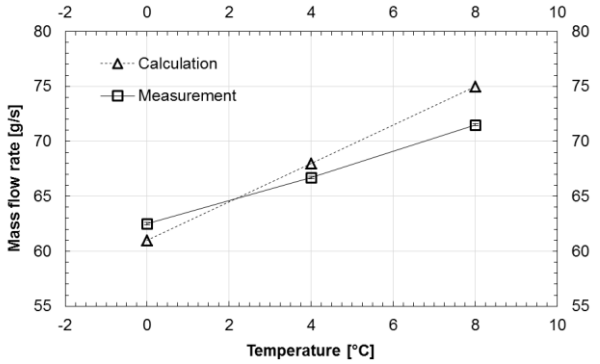

Figure 13: Dependency of the mass flow rate on the coolant temperature of the condenser.

SUMMARY

A multipurpose test facility for supercritical CO_2 has been built. Variable test sections, which can be exchanged easily, allow various experiments for fundamental and applied research, especially in the field of the validation of numerical models for turbulent flow with heat transfer, e.g. in compact heat exchangers in supercritical carbon dioxide. The test facility is designed as closed loop, which delivers a CO_2 mass flow up to 0.110 kg/s to the test section with a maximum pressure of 12 MPa. The test temperature can be set from 5 to 150°C. Depending on this temperature, the transferred thermal power of the facility can raise up to 50 kW.

A decentral PID controlling is implemented to enable stable values of test temperature, pressure and mass flow. A zero dimensional model of the test facility was used to design the facility and the targeted stationary operating points. The data calculated with the help of this model show sufficient congruence with experimental ones.

NOMENCLATURE

A	heat transferring area, m²
A_{pipe}	cross sectional area of pipe, m²
c_p	isobaric heat capacity, J/kg K
d_i	inner diameter, m
$e(k)$	control deviation discrete, Pa or kg/s
$e(t)$	control deviation time-continuous, Pa or kg/s
f	Darcy friction factor
f_c	frequency of the 3-phase current, Hz
F_{set}	setpoint of mass flow rate, kg/s
$h_{in/out}$	specific enthalpy at inlet/outlet; J/kg
k_{layer}	heat conductivity of the boundary layer, W/m K
K_p	proportional control amplification, -
K_v	flow coefficient of expansion valve, m²
L	length, m
m	number of magnetic poles, -
$m_{LP/HP}$	mass on low pressure/high pressure side, kg
$\dot{m}_{sCO_2}$	mass flow rate, kg/s
n	rotational speed, 1/s
p	pressure, Pa
p_0	pressure on low pressure side, Pa
p_1	pressure on high pressure side, Pa
P_{cool}	cooling power, W
P_{set}	setpoint of pressure, Pa
$\dot{Q}$	heat transfer rate, W
$\dot{Q}_{gc}$	heat transfer rate dissipated at gascooler, W
t	time, s
T	temperature, °C
T_{cond}	temperature of condenser cooling fluid, °C
T_N	reset-time, s
T_s	suction gas temperature, °C
T_{vh}	lead-time, s

DOI: 10.17185/duepublico/46081

$u(k)$	set-value discrete, - or Hz
$u(t)$	set value time-continuous, - or Hz
V_{LP}	volume of low pressure side, m³
V_{HP}	volume of high pressure side, m³
V_{pd}	volume of piston displacement, m³

Greek Letters

α	heat transfer coefficient, W/m² K
Δp_{EV}	pressure drop in expansion valve, Pa
Δp_{Pipe}	pressure drop in pipe, Pa
Δt	cycle time, s
η	dynamic viscosity, Pa s
Θ_{log}	mean logarithmic temperature, K
λ	delivery rate
Π	pressure ratio; $\left(\frac{p_1}{p_0}\right)$
ρ	density, kg/m³
ρ_{LP}	density on low pressure side, kg/m³
ρ_{HP}	density on high pressure side, kg/m³
ρ_0	density at compressor inlet, kg/m³
ρ_m	mean density, kg/m³

Non-Dimensional Numbers

Nu	Nusselt number; $\left(\frac{\alpha \cdot d_i}{k_{layer}}\right)$
Pr	Prandtl number; $\left(\frac{\eta}{c_p \cdot k_{layer}}\right)$
Re	Reynolds number; $\left(\frac{\dot{m}_{sCO_2} \cdot d_i}{A_{pipe} \cdot \eta}\right)$

Subscripts

amb	ambient
cool	cooling
cond	condenser
EV	expansion valve
gc	gas cooler
HP	high pressure side
i	inner
in	inlet
layer	boundary layer
log	logarithmic
LP	low pressure side
m	mean
N	reset time
out	outlet
P	proportional
pd	piston displacement
pipe	pipe
sCO_2	supercritical carbon dioxide
set	setpoint
v	valve
vh	lead time

Acronyms and Abbreviations

CAD	Computer Aided Design
CP	Critical Point
DBHE	Diffusion Bonded Heat Exchanger
DIN	Deutsches Institut für Normung
IKE	Institut für Kernenergetik und Energiesysteme
Pt-100	100 Ohm Platin resistance thermometer
SCARLETT	Supercritical CARbon dioxide Loop at IKE Universität StuTTgart
(s)CO_2	(supercritical) Carbon Dioxide
TRGS	Technische Regeln für GefahrStoffe, Guideline for dangerous Substances
TÜV	Technischer ÜberwachungsVerein, German Technical Control Board

ACKNOWLEDGEMENTS

This work was supported by a grant from the Ministry of Science, Research and the Arts of Baden-Württemberg (Az: 32-7533.-8-112/81) to Wolfgang Flaig. and by Deutsche Forschungsgemeinschaft (DFG).

The project leading to this application has received funding from the Euratom research and training programme 2014-2018 under grant agreement No 662116.

REFERENCES

[1] Verein Deutscher Ingenieure (VDI), VDI-Wärmeatlas, Düsseldorf: VDI-Verlag, 2013.

[2] M. E. Shitsman, "Impairment of the Transmission at Supercritical Pressures," *Teplofizika Vysokih Temperature*, vol. 1, no. 4, pp. 237-244, 1963.

[3] B. S. Shiralkar and P. Griffith, "Detoriation in heat transfer to fluids at supercritical pressures and high heat fluxes," *J. Heat Transfer, Trans. ASME,* vol. 91, no. 1, pp. 27-36, 1969.

[4] J. D. Jackson and W. B. Hall, "Forced Convection Heat Transfer to Fluids at Supercritical Pressues," *Turbulent Forced Convection in Channels and Bundles,* pp. 563-611, 1979.

[5] V. G. Razumovskiy, A. P. Ornatskiy and Y. M. Mayevskiy, "Local Heat Transfer and Hydraulic Behavior in Turbulent Channel Flow of Water at Supercritical Pressure," *Heat Transfer Soviet Research,* vol. 22, pp. 91-102, 1990.

[6] V. Dostal, M. Driscoll and P. Heijzlar, "A Supercritical Carbon Dioxide Cycle for Next Generation Nuclear Reactors," MIT- ANP-TR-100, Cambridge, Massachusetts, USA, 2004.

DOI: 10.17185/duepublico/46081

[7] J. Venker, "A Passive Heat Removal Retrofit for BWR's," *Nuclear Engineering International*, vol. 58, pp. 14-17, 2013.

[8] N. Tsuzuki, Y. Kato and T. Ishiduka, "High Performance Printed Circuit Heat Exchanger," *Applied Thermal Engineering*, vol. 27, no. 10, pp. 1702-1707, 2007.

[9] S. Pitla, E. A. Groll and S. Ramadhyani, "New Correlation to Predict the Heat Transfer Coefficient During In-Tube Cooling of Turbulent Supercritical CO2," *International Journal of Refrigeration*, vol. 25, no. 7, pp. 887-895, 2002.

[10] S. H. Yoon, J. H. Kim, Y. W. Hwang, M. S. Kim, K. Min and Y. Kim , "Heat Transfer and Pressure Drop Characteristics During the In-Tube Cooling Process of Carbon Dioxide in the Supercritical Region," *International Journal of Refrigeration*, vol. 26, no. 8, pp. 857-864, 2003.

[11] R. Le Pierres, D. Southall and S. Osborne, "Impact of Mechanical Design Issues on Printed Circuit Heat Exchangers," in *Proceedings of sCO2 Power Cycle Symposium 2011*, Boulder, CO, USA, May 24-25 2011.

[12] A. Kruizenga , M. Anderson, R. Fatima, M. Corradini, A. Towne and R. Devesh, "Heat Transfer of Supercritical Carbon Dioxide in Printed Circuit Heat Exchanger Geometries," *ASME Journal of Thermal Science and Engineering Applications*, vol. 3, no. 3, p. 031002, 2011.

[13] S. H. Song, H. Y. Kim, H. Kim and Y. Y. Bae, "Heat Transfer Characteristics of a Supercritical Fluid Flow in a Vertical Pipe," *Journal of Supercritical Fluids*, vol. 44, no. 2, pp. 164-171, 2008.

[14] P. C. Simoes, J. Fernandes and J. P. Mota, "Dynamic Model Supercritical Carbon Dioxid Heat Exchanger," *Journal of Supercritical Fluids*, vol. 35, no. 2, p. 2005, 167-173.

[15] M. D. Carlson, A. Kruizenga , M. Anderson and M. Corradini, "Measurements of Heat Transfer and Pressure Drop Characteristics of Supercritical Carbon Dioxide Flowing in Zig-Zag Printed Circuit Heat Exchanger Channels," in *Supercritical CO2 Power Cycle Symposium*, Boulder, Colorado, USA, May 24-25, 2011.

[16] S. A. Wright, R. F. Radel, M. E. Vernon, G. E. Rochau and P. S. Pickard, "Operation and Analysis of a Supercritical CO2 Brayton Cycle," Sandia National Laboratories, Albuquerque, New Mexico, USA, 2010.

[17] B. T. Swapnalee, P. K. Vijayan, M. Sharma and D. S. Pilkhwal, "Steady State Flow and Static Instability of Supercritical Natural Circulation Loops," *Nuclear Engineering and Design*, vol. 245, pp. 99-112, 2012.

[18] Deutsches Institut für Normung (DIN), "Unbefeuerte Druckbehälter-Teil 3: Konstruktion," Beuth Verlag, No. EN 13445-3:2011-2, Berlin, 2011.

[19] C. Dang, K. Hoshika and E. Hihara, "Effect of lubricating oil on the flow and heat-transfer characteristics of supercritical carbon dioxide," *International Journal of Refigeration*, vol. 35, pp. 1410-1417, 2012.

[20] Bundesministerium für Arbeit und Soziales, Technische Regeln für Gefahrstoffe, TRGS 900, Berlin: Gemeinsames Ministerialblatt BArBl, 2006.

[21] Das Europäische Parlament und der Rat der Europäischen Union, Richtlinie 97/23/EG des Europäischen Parlaments und des Rates vom 29. Mai 1997 zur Angleichung der Rechtsvorschriften der Mitgliedsstaaten über Druckgeräte, Brüssel: ABl 181, 1997.

[22] Deutsches Institut für Normung (DIN), "Kälteanlagen und Wärmepumpen-Sicherheitstechnische und Umweltrelevante anforderungen," Beuth Verlag, EN 378-1:2008+A2:2012, Berlin, 2012.

DOI: 10.17185/duepublico/46081